Characterization of gas pipeline flaws using wavelet analysis

Raymond W. Tucker, Jr. [a], Stephen W. Kercel [a], Venugopal K. Varma [b]
[a] Engineering Science and Technology Div., Oak Ridge National Laboratory, Oak Ridge, TN 37831
[b] Nuclear Science and Technology Div., Oak Ridge National Laboratory, Oak Ridge, TN 37831

ABSTRACT

As U.S. natural gas supply pipelines are aging, non-destructive inspection techniques are needed to maintain the integrity and reliability of the natural gas supply infrastructure. Ultrasonic waves are one promising method for non-destructive inspection of pipeline integrity. As the waves travel through the pipe wall, they are affected by the features they encounter. In order to build a practical inspection system that uses ultrasonic waves, an analysis method is needed that can distinguish between normal pipe wall features, such as welds, and potentially serious flaws, such as cracks and corrosion. Ideally, the determination between "flaw" and "no-flaw" must be made in real-time as the inspection system passes through the pipe. Because wavelet basis functions share some common traits with ultrasonic waves, wavelet analysis is particularly well-suited for this application. Using relatively simple features derived from the wavelet analysis of ultrasonic wave signatures traveling in a pipe wall, we have successfully demonstrated the ability to distinguish between the "flaw" and "no-flaw" classes of ultrasonic signatures.

Keywords: flaw detection, wavelets, ultrasonic waves, EMAT, pipeline inspection

1. NON-DESTRUCTIVE TESTING OF GAS PIPELINES

Approximately 30% of the energy produced in the United States is derived from natural gas. Accordingly, the integrity of the natural gas supply system is of prime importance. Natural gas is supplied to users through a vast pipeline network that consists of over a million miles of pipeline.[1] Pipeline companies have an impressive safety record due to the proactive role they have taken in establishing standards and in the inspection of pipelines. Many of the pipelines are getting old, and there is a great need for a way to identify cracks, corrosion, and other defects that can potentially cause problems.

A gas pipeline can fail due to many causes. Some of the most common failure modes are corrosion, pitting, stress corrosion cracks, seam weld cracks, dents, and other flaws induced by external impact from earth-moving equipment. Ideally, it would be desirable to detect all of the above flaw types with a single inspection technique. Unfortunately, there is no one inspection technique that is ideally suited to detect all of the possible flaw types. Hence, the gas industry uses a combination of techniques to ensure the safety margin for their operation. Probabilistic approaches have been used for estimating pipeline integrity.[2] Probabilistic methods attempt to predict safety using crack rate growth data, inspection frequency data, and the operating parameters of the pipe. Probabilistic methods, however, require valid statistical data on flaw rate occurrences and distributions to be of any real use. Hence, the need persists to be able to collect accurate data on the actual condition of the pipelines in service.

There are two main methods of testing the integrity of pipelines; destructive inspection and non-destructive inspection (NDI.) The destructive inspection procedure generally uses a hydrostatic technique to verify that the pipeline integrity is within the safety margin for operation. The procedure does not, however, locate defects that are just below the threshold of safety. In addition, destructive testing disrupts the pipeline's normal operation. For this reason it is not the preferred method. Generally, such techniques are good for the initial inspection of pipelines before they are put into use. On the other hand, NDI techniques can detect developing flaws that can cause failures in the future. Thus, NDI provides a quantitative measure of the integrity of the pipeline as well as a measure of its current safety margin.

Some types of defects that can occur in pipelines are a serious threat to the safety of the pipeline. Stress corrosion cracking, for example, can occur at any time in the life of the pipeline, and it occurs under a broad range of field

conditions. This type of defect is usually oriented along the axial (lengthwise) direction of the pipe. If not detected early, the cracks may grow and/or coalesce, eventually resulting in a leak or rupture of the pipe. Not all defects that develop in pipelines threaten the integrity of the pipeline. Benign, internal inclusions are common and do not pose a serious threat to the integrity of the pipeline. NDI systems are urgently needed that can (1) provide early detection of the more serious defects; (2) differentiate between the serious defects and benign inclusions; and (3) characterize the type and size of the defects for repair or replacement management.

The two most common NDI methods for testing pipelines are the magnetic flux leakage (MFL) method and the ultrasonic guided wave method. The MFL method applies a localized magnetic field on the inside of the pipe wall. Disruptions in the local magnetic field are presumed to be caused by disturbances (flaws) in the pipe wall. When corrosion or other degradation of the pipe wall occurs, the pipe wall thickness is effectively reduced. At these locations, the amount of magnetic flux reaching the sensor is also reduced.[3] Cracks in the pipe wall can also potentially cause flux leakage. However, the ability of the MFL technique to detect cracks is somewhat sensitive to the orientation of the flux lines in the pipe wall. For example, an MFL system that employs flux lines that are parallel to the axis of the pipe can detect corrosion and dents, but cannot detect axial stress corrosion cracks or seam weld cracks. Detection of these flaws requires a second MFL system with the flux lines oriented in the transverse rather than the axial direction.[4] Recent research related to the MFL method has focused on variations in sensor type and configuration, and in the interpretation of the data for defect sizing and classification.[5,6]

A promising alternative to the MFL method is the use of guided ultrasonic waves for detecting the defects that occur in pipelines. One major benefit of ultrasonic guided waves is their ability to travel longer distances in the pipe wall, which enables them to inspect the structure line-by-line instead of point-by-point. As the guided waves travel through the pipe walls, they are affected by the features they encounter. In particular, the mode structure of the propagating ultrasonic wave is modified in specific ways depending on the specific flaw type encountered by the wave. The received signals contain much information regarding the nature and sizing of the features encountered. However, defect detection, classification, and sizing using guided ultrasonic waves is still a major challenge under investigation due to the complexity of the wave propagation characteristics. A major shortcoming of many of the previous investigations into the use of ultrasonic guided waves has been the lack of a suitable signal analysis method to adequately identify the mode conversion produced in the ultrasonic wave by the flaw.

This paper summarizes a preliminary investigation into the use of the discrete wavelet transform as the underlying methodology for flaw detection using ultrasonic guided waves. We first briefly describe the generation and detection of ultrasonic waves using electromagnetic acoustic transducers (EMAT's.) We then describe the experimental apparatus used to collect the data. We briefly discuss the characteristics of wavelets that make them particularly suitable for addressing the problem at hand, and then report the results obtained to date using wavelet analysis. We conclude by suggesting a possible way to extend the analysis to include the classification of flaws by type.

2. ULTRASONIC WAVE GENERATION AND DETECTION USING EMATS

A common method for inducing ultrasonic guided waves in pipe walls is to use an electromagnetic acoustic transducer (EMAT.) Since the EMAT transducer does not have to be in physical contact with the pipe wall to induce ultrasonic waves, it is particularly well suited for pipeline inspection. The EMAT consists of a strong permanent magnet with a coil of wire located between the magnet and the pipe wall. The permanent magnet creates a static electromagnetic field that extends in a direction perpendicular to the surface of the pipe wall. When a gated, high-current sinusoidal pulse is passed through the EMAT coil, a dynamic field is created that is parallel to the pipe wall and perpendicular to the static field. The interaction of the static field and oscillating dynamic field generates magnetostrictive forces within the surface of the pipe. The forces acting on the surface can generate lamb, shear, and longitudinal ultrasonic waves in the pipe wall, depending on the configuration of the magnet and the characteristics of the current flow.[7] These waves can propagate over relatively long distances in the pipe wall. Figure 1 illustrates the use of EMAT's for pipeline inspection. In this configuration, one EMAT serves to generate the ultrasonic wave, while the other acts as the receiver (sensor). Figure 1 illustrates the two EMAT's in a *transmission mode* configuration, where the ultrasonic wave travels from a source EMAT through the flaw on its way to a separate EMAT used as a sensor. It is also possible to perform

measurements of this type in a *reflection mode* using a single EMAT as both source and sensor. In this mode of operation, the received signal is actually a partial reflection of the ultrasonic wave created by the interaction of the wave with the flaw. All measurements used in this work were obtained using the transmission mode configuration. By using the through transmission mode whereby the distance between the EMAT's is fixed, better correlation was obtained for the effect of flaws.

There have been many studies devoted to understanding the generation and propagation characteristics of the different ultrasonic wave types in media such as pipe walls.[8,9,10,11,12] Shear horizontal (SH) waves have demonstrated their suitability for use in pipeline inspection because of their simpler dispersion characteristics and their tolerance of the damping caused by the protective coating present on the inner surface of many gas pipelines.[8] It is also desirable to avoid generating multiple wave modes, since this greatly complicates both the interaction of the waves with the defects and the signal analysis required to interpret the results. Most of the tests for this study were performed using the n1 mode SH wave. The particular wave mode induced is dependent upon the frequency of the current signal that is passed through the EMAT conductor.

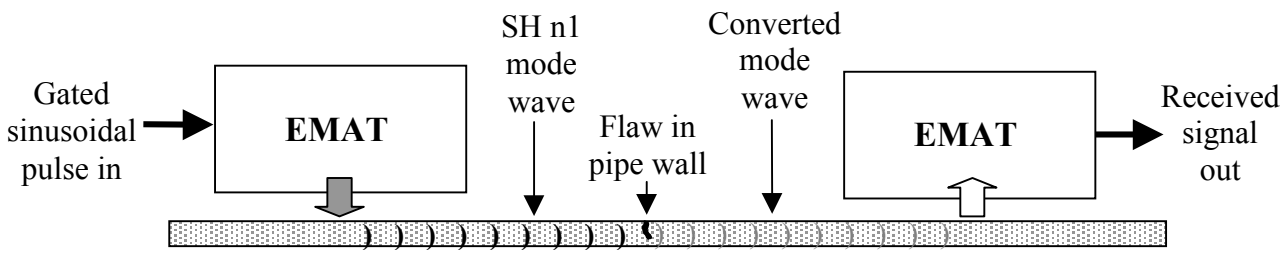

Figure 1. Illustration of through transmission mode ultrasonic wave generation using EMAT's.

3. EXPERIMENTAL SETUP

Six-foot lengths of 10-inch and 12-inch pipe were obtained for use in collecting the experimental data. To simulate the presence of cracks in the pipe wall, 0.25-inch-, 0.125-inch-, and 0.006-inch-wide grooves of varying depths were machined in both the axial and circumferential directions in the pipe walls. The simulated flaws were separated spatially from the end of the pipe and from each other by several times the spacing between the transmitter and receiver EMAT's. This was done to allow collection of ultrasonic wave signatures containing a minimum number of reflections from pipe wall features other than the immediate flaw of interest. In additional, a short length of used 10-inch pipe containing stress corrosion cracking was obtained to allow the collection of data representative of that flaw type.

The EMAT transducers used were designed to fit the inside radius of both the 10-inch and 12-inch pipe. Hardware fixtures were designed and fabricated for allowing the EMAT's to be positioned and traversed along the inside walls of the pipe. The mounting fixtures also had provisions to vary the gap between the pipe wall and the EMAT's. The EMAT/fixture assembly was held in place by the strong permanent magnet within the EMAT. Figure 2 shows the transmitter/receiver EMAT pair in both the circumferential and axial geometries. The circumferentially-oriented EMAT pair shown on the left was used to detect flaws oriented in the axial direction, while the axially-oriented pair shown on the right was used to detect flaws and weld defects in the circumferential direction.

The EMAT excitation signal was provided by a programmable amplifier/receiver module capable of delivering a gated, high voltage RF pulse to the transmitter EMAT. The amplifier/receiver module was also equipped with a broadband receiver amplifier which was used to amplify the signal from the receiver EMAT. The resulting signal was lowpass filtered and sampled using an analog-to-digital converter. The received signals were recorded on disk and analyzed offline. Data were collected on sections of the pipe known to be free of flaws as well as on the sections containing the flaws. A sample of the windowed receiver signal for both the flaw and no-flaw case is shown in Figure 3. As can be seen from the figure, the signal is strongest when there is no flaw. The signature is reduced in amplitude when it

encounters a flaw. Despite the fact that such changes are obvious in laboratory data collected under carefully controlled conditions, changes in the received signal amplitude in the time domain data (see Figure 3) are not a useful feature for identifying flaws in less controlled field conditions. In actual pipelines, there are other mechanisms besides a flaw that

Figure 2. EMAT test fixtures used to collect experimental data. The circumferentially-oriented pair on the left was used to detect cracks in the axial direction. The axially-oriented pair on the right was used to detect cracks in the circumferential direction.

can lead to attenuation of the signal. The necessary set of features for flaw detection are those that depend on the mode conversion imposed by the flaw as observed in the shape of the received signal. Thus, the goal of the signal processing effort was to identify features that can differentiate between the "flaw" and "no-flaw" cases based on the shape rather than the amplitude of the received pulse.

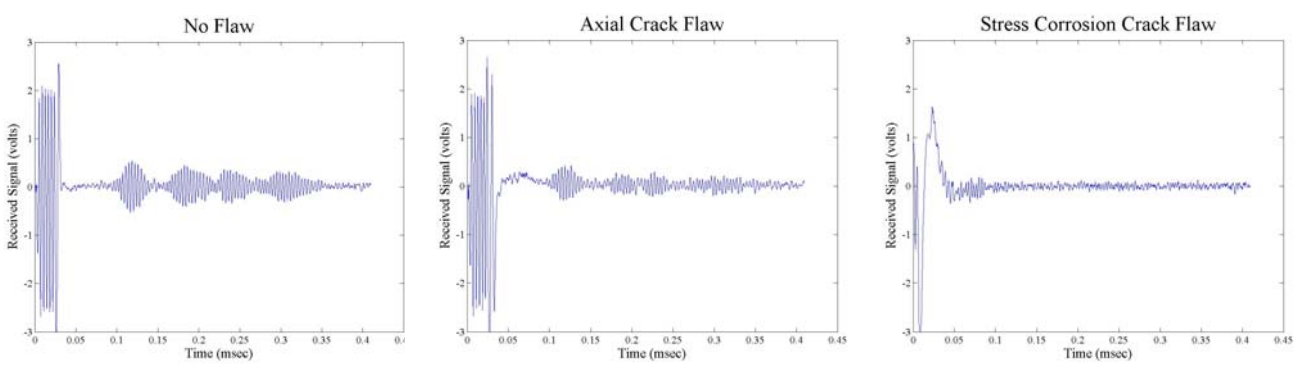

(a) **(b)** **(c)**

Figure 3. Received signals indicating the (a) flaw; (b) axial crack flaw; and (c) stress corrosion crack flaw conditions.

4. ADVANTAGES OF WAVELET ANALYSIS FOR PIPELINE INSPECTION

A common approach used in signal analysis is to employ a transform method that represents the signal to be analyzed as a weighted sum of variations of a simpler signal with known properties. The simpler signal is mathematically referred to as the *basis function*. The values assigned to the resulting weights often reveal information that is not evident in the original signal. For example, in the popular case of Fourier analysis, the underlying basis function is the familiar

sinusoid. The signal is represented as a weighted sum of sinusoids (sines and cosines) at different frequencies. The weights in this case correspond to a measure of the signal energy present at the particular frequency associated with the weight. For many applications, the relative values of the weights allow the extraction of useful information (features) that can be used in pattern recognition algorithms to characterize fault conditions. For example, a flat spot on a motor bearing would cause an increase in the signal energy at a particular frequency (and perhaps its harmonics) in the vibration signature for the motor. In Fourier analysis, this would correspond to an increase in the weight assigned to that particular frequency (and its harmonics) in the transformed signal. To detect a bad bearing, the weight for that particular frequency could be used as a simple feature. If the value of the feature exceeded a simple threshold, the bearing could be classified as "bad."

While Fourier analysis is useful in many instances, it is not well suited for all signal analysis applications. As previously pointed out, the basis functions used in Fourier analysis are sines and cosines at different frequencies. By definition, sines and cosines are infinite in length. Since it is impossible to record a signal of infinite length, the Fourier transform by its nature attempts to represent a finite-length signal as the sum of a set of infinite functions. For signals whose statistical properties have little or no variation over long time periods (such as the motor vibration signature mentioned above), this characteristic does not represent a serious limitation. However, for transient signals that are by nature short in duration, the sinusoid is not necessarily the best choice of basis functions available. The reason that Fourier analysis is awkward in these cases is that most (but not quite all) of the coefficient weights must be assigned such that all of the infinite sinusoids cancel exactly when summed.

As previously discussed, the EMAT-induced ultrasonic wave is an oscillating, transient burst of energy. The goal of the signal analysis effort is to determine how a flaw in the pipe wall disrupts the shape of that burst. A reasonable signal analysis approach would be to represent the signal using basis functions that are themselves oscillating, transient bursts. The most useful technique for performing such an analysis is the discrete wavelet transform. Wavelet basis functions have a number of mathematical properties that make them well-suited for analyzing transient signals. The first of these properties is that the wavelet basis function must have zero average value; hence it must oscillate. The second important property is that it must have finite energy; hence it must be a windowed burst. Since wavelet basis functions and ultrasonic wave signals share these properties, the weights that result from the wavelet transform should be useful in discriminating different flaw conditions within the pipe wall. An example of a useful wavelet basis function, $\psi(t)$, is shown in Figure 4. A discrete wavelet basis function such as the one shown in Figure 4 represents a complete basis for any real-valued function f(t), except for f(t) = a constant. In other words, any non-constant, real-valued function (i.e., measured signal) can be completely described as the weighted sum of scaled and shifted versions of $\psi(t)$. The discrete wavelet transform is the list of real-valued weights from that weighted sum.

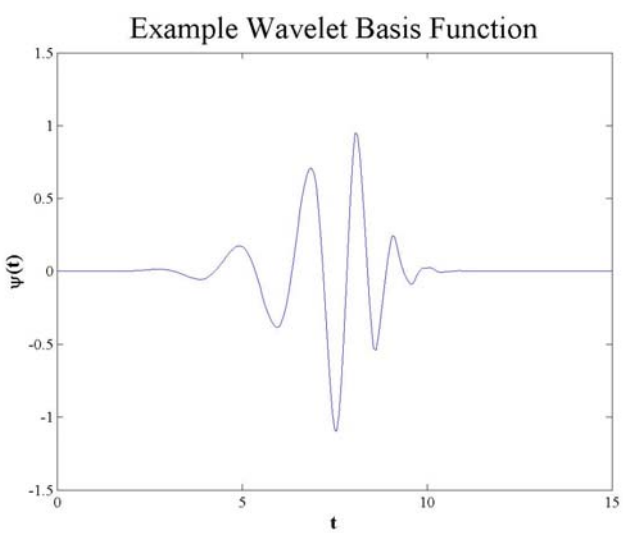

Figure 4. Example wavelet basis function. The wavelet basis function shown is the Daubechies 8-coefficient wavelet.

In computing the discrete wavelet transform, the base wavelet is repeatedly scaled by a factor of 2. This operation produces a number of “scales” in the resulting transform. The weights in each successive scale contain a relative measure of the similarity of the scaled wavelet basis function to the original signal. All of the wavelet basis functions used for this application also have the mathematical property of orthogonality. This property guarantees that all of the energy (or information) in the signal is distributed among the different wavelet scales such that no energy (or information) is lost, and there is no overlap of energy between scales.

By comparing the representative ultrasonic wave signal in Figure 3 with the wavelet basis function in Figure 4, it is easy to visualize that there will be certain scales at which the wavelet basis function will be very similar to the ultrasonic wave signal. It is also easy to visualize that at other scales, the similarity will be small. In general, when the discrete wavelet transform is computed for a transient signal, most of the energy (or information) is contained in a few large weights. In applications where the weights are used as features for pattern recognition purposes, this characteristic can help reduce the dimensionality of the feature vector, thereby simplifying the implementation of the classifier.

5. FLAW DETECTION USING WAVELET ANALYSIS

For pipeline inspection using ultrasonic waves, the signal processing methodology must address two distinct problems. The first problem is to distinguish between the true flaws and normal pipeline features, such as welds, bends, coatings, and benign inclusions. The second (and more difficult) problem is to actually classify the flaw signatures by type and size. To construct a practical inspection system, the "flaw" versus "no-flaw" classification must be done in real-time as the inspection platform (known as a “pig”) moves along the inside of the pipeline. This requirement is dictated by the fact that when the pig is running down the pipe, it collects hundreds of ultrasonic signatures per second. Each signature is a vector of several hundred to several thousand discrete samples. The pig typically travels through the pipe at a velocity of 2-10 feet per second for tens to hundreds of miles without human intervention. It would not be feasible to store all the raw signature data collected during the run for post-processing. Thus, at minimum, the on-board processor must be able to identify the "flaw" signatures in real-time and store them while discarding the "no-flaw" signatures.

To determine if the “flaw” versus “no-flaw” classification is feasible in real-time, a discrete wavelet analysis was performed on the data collected from the 10- and 12-inch diameter pipes with fabricated flaws and the shorter 10-inch pipe section with stress corrosion cracking. For the experimental data collected thus far, a method has been devised for each pipe and flaw type to correctly classify the “flaw” versus “no-flaw” signatures. The features used to distinguish between the two classes of signatures have been the energies and entropies on various wavelet or wavelet packet scales. The energy on a wavelet scale is computed by taking the inner product of the list of wavelet coefficients on the scale with itself. Entropy is the Shannon entropy from information theory. Since it measures the tendency of a signal to form peaks, it can be an indication as to the extent a signal is concentrated or spread out in time.

The signatures for axial flaw data for the 12-inch pipe were successfully classified using the following procedure. The wavelet basis function used was a 20-coefficient Daubechies Wavelet. A “best-basis” wavelet-packet transform of the input signal was computed. As expected, the wavelet transform result was dominated by a few large coefficients spread over the first few wavelet scales. To simplify the computation, only the largest coefficients (those representing approximately 90% of the total signal energy) were retained for the analysis. The smaller coefficients were set to zero. The entropies of the larger coefficients for wavelet packet scales 2, 3, and 4 were computed, yielding a feature vector consisting of three numbers. The two classes (flawed and unflawed) were separable within the three-dimensional feature space. The entropies of the larger coefficients for wavelet-packet scales 2 and 3 were also computed, yielding a two-dimensional feature vector for each trial. The two classes (flawed and unflawed) were also separable in the two-dimensional feature space, but over a narrower range of retained energies than for the three-dimensional feature vector. Signatures for the circumferential flaw data for the 12-inch pipe were fully distinguished by an analysis similar to that described above. The wavelet basis function used for processing the circumferential signatures was a 78-coefficient Coiflet. The two-dimensional feature vector was computed from the entropies of wavelet-packet scales 2 and 3.

Signatures for the 10-inch pipe were fully distinguished into three classes (no flaw, single flaw, and multiple flaws) by an analysis similar to that described above. The wavelet basis function used for processing was an 8-coefficient Least Asymmetric Wavelet. As before, only the larger coefficients were retained for the analysis. The entropies of the larger coefficients for wavelet packet scales 2, 3, 4 and 5 were computed, yielding a four-dimensional feature vector for each trial.

Figures 5-7 illustrate the results for each of the cases described above. In each plot, the horizontal axis is the fraction of signal energy retained in wavelet-packet space for the analysis. The vertical axis is the $\log_{10}$ of the square of the Mahalanobis distance of the feature vector from the cluster center of the "no flaw" samples. The “no flaw” cluster center was determined by computing the mean of a large set of feature vectors representing the “no flaw” case. There is one line on the graph for each trial. The line represents a measure of the distance of the feature vector from the "no flaw" cluster center as a function of retained energy. The log scale was used to generate the graphs simply as a matter of convenience.

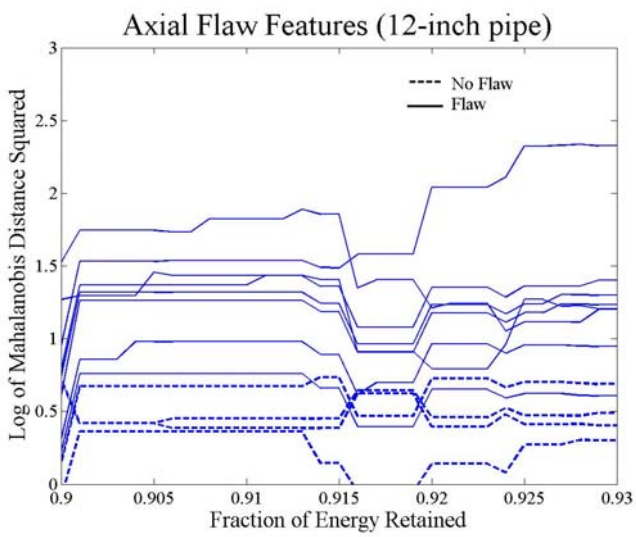

Figure 5. Distinction of axial flaw features for 12-inch pipe.

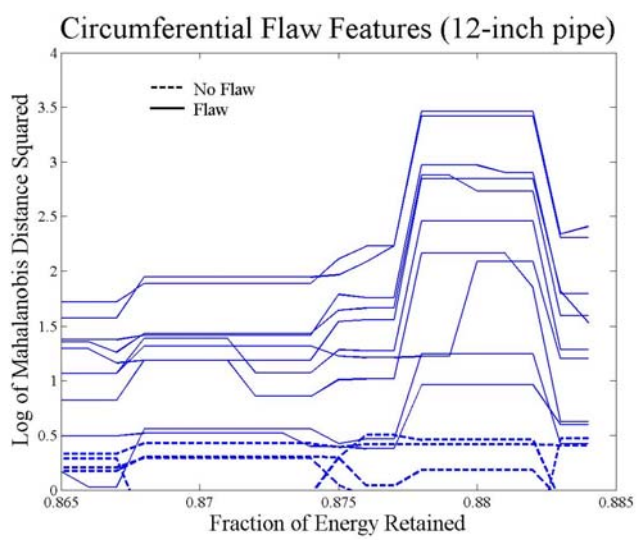

Figure 6. Distinction of circumferential flaw features for 12-inch pipe.

Signatures for the stress corrosion crack samples were also readily distinguishable from non-corroded samples using a two-dimensional feature vector. The wavelet basis function used was the Daubechies 10-coefficient least asymmetric wavelet in a wavelet packet transform. The first feature was the fraction of the total signal energy contained in the two wavelet packet levels having the highest total energies. This is a measure of the concentration of the signal in the wavelet scale domain. The other feature was the sum of the entropies of all the levels in wavelet packet space after the smallest coefficients containing 10% of the signal energy were zeroed out; this is a measure of the concentration of the signal in the time domain.

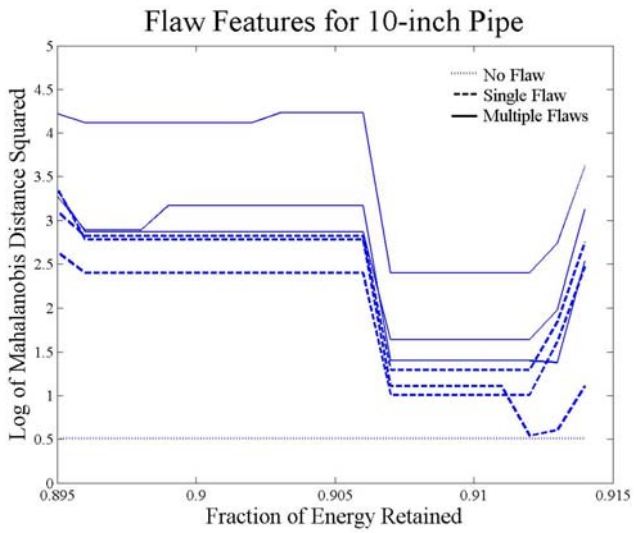

Figure 7. Distinction of flaw feature for 10-inch pipe.

6. CONCLUSIONS

For each flaw type and pipe size, we have been able to find features derived using wavelet analysis that allow us to distinguish between "flaw" and "no-flaw" ultrasonic signatures. For each flaw type, the computation is simple enough that it can be implemented in a real-time inspection system on the pig using existing microprocessor technology. Since the vast majority of the signatures collected by the inspection system will be the "no flaw" case, the data storage requirements for the inspection system have been greatly reduced, making the construction of such a system feasible.

Research is ongoing to find a single feature space in which flaws can be readily distinguished from no-flaw signatures. Although it is feasible to use different techniques to extract multiple features vectors as described above to identify different flaw types, it would further simplify the computational load to have a single analysis procedure that reliably distinguishes between flaw and no-flaw signatures.

Ideally, classification by flaw type will also be performed by the inspection system on board the pig. Different flaw types induce conversions of transmitted ultrasonic wave modes in predictable ways. The idealized time domain signature of a given mode is known. Once the presence of the flaw is determined by wavelet analysis, cross correlation can be performed between the idealized exemplar and the measured signal. This calculation should be easily realized in real time using Fourier-based cross correlation, and provide reliable classification by flaw type. There is also a possibility that this analysis will yield specific flaw parameters such as depth of crack, but that would be much more difficult than merely classifying by type.

7. ACKNOWLEDGEMENTS

This work was supported by the DOE National Energy Technology Laboratory (NETL), Strategic Center for Natural Gas. The work was performed at Oak Ridge National Laboratory, which is managed and operated by UT-Battelle, LLC.., for the U.S. Department of Energy under Contract No. DE-AC05-00OR22725.

The authors would also like to thank Dr. Joseph Rose of Pennsylvania State University for his guidance in understanding the physical phenomena that occurs during ultrasonic wave propagation.

REFERENCES

1. Posakony, G.J., and Hill, V.L., "Assuring the integrity of natural gas transmission pipelines," Topical Report, Gas Research Institute, GRI-91/0366, November 1992.
2. Khaleel, M.A., and Simonen, F.A., "Effects of alternative inspection strategies on piping reliability," *Nuclear Engineering and Design*, Vol. 197, pp. 115-140, April 2000.
3. Rosen, H., and Lewis, R., "Improved magnetic flux pipeline inspection tools in practice," *Pipeline Pigging and Inspection Technology Conference*, Houston, TX, February 17-20, 1992.
4. Porter, P.C., "Use of magnetic flux leakage (MFL) for the inspection of pipelines and storage tanks," *Nondestructive Evaluation Of Aging Utilities*, Proceedings of the SPIE, Vol. 2454, Walter G. Reuter, Editor, pp. 172-184, May 1995.
5. Udpa, L., Mandayam, S., Udpa, S., Sun, Y., and Lord, W., "Developments in gas pipeline inspection," *Materials Evaluation*, pp. 467-472, April 1996.
6. Mandayam, S., Udpa, L., Udpa, S., and Lord, W., " Signal processing for inline inspection of gas transmission pipelines," *Research In Nondestructive Evaluation*, Volume 8, No. 4, pp. 233-247, Springer-Verlag, 1996.
7. Thompson, R.B., "Physical Principles of Measurements with EMAT Transducers" *Physical Acoustics*, edited by W. P Mason, Academic Press, Vol. XIX, pp.157-199, 1990.
8. Hirao, M., and Ogi, H., "An SH-wave EMAT technique for gas pipeline inspection," *NDT&E International*, Vol. 32, pp 127-132, 1999.
9. Gauthler, J., Mustafa, V., Chabbaz, A., and Hay, D.R., "EMAT generation of horizontally polarized guided shear waves for ultrasonic inspection," *Proceedings of the International Pipeline Conference*, Vol. 1, ASME, June 1998.
10. Sawaragi, K., Salzburger, H.J., Hubschen, G., Enami, K., Kirihigashi, A., and Tachibana, N., "Improvement of SH-wave EMAT phased array inspection by new eight segment probes," *Nuclear Engineering and Design*, Vol. 198, pp. 153-163, May 2000.
11. Kwun, H., Hanley, J.J., and Holt, A.E., "Detection of corrosion in pipe using magnetostrictive sensor technique," *Nondestructive Evaluation Of Aging Maritime Applications*, Proceedings of the SPIE Vol. 2459, Richard B. Mignogna, Editor, , pp. 140-148, June 1995.
12. Kwun, H., and Hanley, J.J, "NDE of steel Gas pipelines using magnetostrictive sensors," Topical Report, Gas Research Institute, GRI-95/0362, October 1995.